

1 **Seasonal snowpack microbial ecology and biogeochemistry on a High Arctic ice cap
2 reveals negligible autotrophic activity during spring and summer melt**

3 **A. Dayal¹, A.J. Hodson^{2,3}, M. Šabacká⁴ and A. L. Smalley⁵**

4 ¹Institute of Biological, Environmental & Rural Sciences, Aberystwyth University, Aberystwyth,
5 UK. ²Arctic Geology Department, University Centre in Svalbard, Longyearbyen, Norway.

6 ³Department of Environmental Sciences, Western Norway University of Applied Sciences,
7 Sogndal, Norway. ⁴Centre for Polar Ecology, University of South Bohemia, Czech Republic.

8 ⁵Department of Geography, University of Sheffield, UK.

9 Corresponding author: Archana Dayal (ard33@aber.ac.uk)

10 **Key Points:**

- 11
- 12 • Nutrients delivered by snow from marine and continental sources were supplemented by the
13 dissolution of dust deposited from local sources
- 14
- 15 • Autotrophic communities were conspicuous by their absence within a High Arctic glacial
16 snowpack during summer
- 17
- 18 • Secondary bacterial production therefore dominated the entire summer
- 19
- 20 • A superimposed ice layer of refrozen snowmelt acted as a temporary dilute store for nutrients
21 and cells

22 **Abstract**

23 Snowpack ecosystem studies are primarily derived from research on snow-on-soil ecosystems.
24 Greater research attention needs to be directed to the study of glacial snow covers as most snow
25 cover lies on glaciers and ice sheets. With rising temperatures, snowpacks are getting wetter, which
26 can potentially give rise to biologically productive snowpacks. The present study set out to
27 determine the linkage between the thermal evolution of a snowpack and the seasonal microbial
28 ecology of snow. We present the first comprehensive study of the seasonal microbial activity and
29 biogeochemistry within a melting glacial snowpack on a High Arctic ice cap, Foxfonna, in
30 Svalbard. Nutrients from winter atmospheric bulk deposition were supplemented by dust
31 fertilisation and weathering processes. NH_4^+ and PO_4^{3-} resources in the snow therefore reached
32 their highest values during late June and early July, at 22 and 13.9 mg m^{-2} , respectively. However,
33 primary production did not respond to this nutrient resource due to an absence of autotrophs in the
34 snowpack. The average autotrophic abundance on the ice cap throughout the melt season was $0.5 \pm 2.7 \text{ cells mL}^{-1}$. Instead, the microbial cell abundance was dominated by bacterial cells that
35 increased from an average of $(39 \pm 19 \text{ cells mL}^{-1})$ in June to $(363 \pm 595 \text{ cells mL}^{-1})$ in early July.
36 Thus, the total seasonal biological production on Foxfonna was estimated at 153 mg C m^{-2} , and
37 the glacial snowpack microbial ecosystem was identified as net-heterotrophic. This work presents
38 a seasonal 'album' documenting the bacterial ecology of glacial snowpacks.

40 **Plain language summary**

41 Most research attention has been given to snow covers lying on top of soil ecosystems, and
42 therefore we do not know enough about the ecology of glacial snowpack ecosystems. This is a
43 major knowledge gap, given that most of the world's snow cover lies over glaciers, ice caps and
44 ice sheets. This study shows that during the melt season on a High Arctic ice cap, Foxfonna in
45 Svalbard, nutrients are most available during the peak of summer (June to early July transition
46 period), but a shortage of photosynthesising microbes can mean that they largely remain in situ
47 until transported downstream by meltwater runoff. Processes with the capacity to generate high
48 concentrations of essential nutrients such as N and P in snow and meltwater could therefore be
49 described, because the primary producers did not sequester them. In contrast, an increase in
50 bacterial cell numbers was observed during the same period. The glacial snowpack ecosystem was
51 therefore net-heterotrophic due to the absence of autotrophs and proliferation of bacterial cells.
52 Since the nutrient demand of the bacterial biomass is low, the ecosystem releases carbon, nitrogen,
53 and phosphorus, rather than fixes it.

54

55

56

57

58

59

60 1 Introduction

61 1.1 The status of glacier snowpack ecosystem research

62 Seasonal snowpacks cover nearly a third of the Earth's land surface at the start of summer with a
63 mean winter maximum extent of $47 \times 10^6 \text{ km}^2$ (Hinkler *et al.*, 2008). Snow covers play an integral
64 role in the climate system via radiative feedbacks, ground insulation (Hinkler *et al.*, 2008) and
65 biogeochemical cycles (Wadham *et al.*, 2013). Although snowpacks have received significant
66 research attention, most has been in the context of snow covers lying on top of soil or other aquatic
67 ecosystems (Jones *et al.*, 1999; Kuhn, 2001; Larose *et al.*, 2010; Larose, Dommergue and Vogel,
68 2013).

69
70 What is known about glacial snowpack ecosystems is largely derived from molecular, functional,
71 and physiological studies (e.g., Lutz *et al.*, 2016; Malard *et al.* 2019; Hoham and Remias, 2020).
72 These studies have given a great deal of attention to snow algae and glacier algae, not least due to
73 their linkage with pigment-mediated albedo reduction and melt enhancement (Williamson *et al.*,
74 2019; Cook *et al.*, 2020; Gray *et al.*, 2020; Mauro *et al.*, 2020). Recently, there has been a shift
75 from the aforementioned studies to the study of interactions between algae, fungi and bacteria
76 (Krug *et al.*, 2020; Fiołka *et al.*, 2021). Although important, such approaches have offered little
77 understanding of fundamental ecosystem characteristics, such as links to biogeochemical
78 processes and the changing physical conditions of a snowpack during melt.
79

80 We are yet to understand the (re)distribution of nutrients and microbes within the different layers
81 of a melting snowpack and how this supports the concept of the snowpack as an ecosystem,
82 especially in the context of changing climate. From this perspective, it is expected that surface
83 meltwater will play a critical role in the redistribution of microbes and nutrients on the surface of
84 glaciers, including their delivery to the deeper (darker) layers of the snowpack or the glacier bed,
85 where photosynthesis cannot occur, and heterotrophic production is likely to be dominant (e.g.,
86 (Skidmore *et al.*, 2000; Mikucki and Priscu, 2007). Additionally, one can expect the ecology of
87 snow to be driven by the production of meltwater and the changes in the snowpack's physical
88 condition during melt because this greatly affects the propagation of light through the snow and
89 the transfer of nutrients by percolating liquid water (e.g. Tranter and Jones, 2001; Hodson *et al.*,
90 2017). We, therefore, hypothesise that with the evolution in a snowpack's physical condition
91 during summer melt, greater heterogeneity will be expected in microbial abundance and nutrients
92 within the different layers of a melting snowpack (see also Nowak *et al.*, 2018).
93

94 In addition to increased melting, the warming of the cryosphere is also changing the composition
95 of snowpacks. For example, a surface energy/mass balance model of an Arctic glacier (Wright *et*
96 *al.*, 2007) predicted that due to rising temperatures, superimposed ice (formed following the
97 refreezing of meltwater) will account for greater than 50% of the total accumulation by 2050.
98 Furthermore, this superimposed ice has been shown to be a transient reservoir of nutrients/organic
99 carbon in an earlier study on the Foxfonna ice cap (Kozioł *et al.*, 2014, 2019). In addition, Hell *et*
100 *al.*, 2013 demonstrated that the microbial communities within the melting snowpack were
101 structured according to habitat type, i.e., most taxa showed different distributions based on the
102 habitat (surface snow, snow, slush and near-surface ice). This niche specificity was also
103 demonstrated in a maritime Antarctic (Livingston Island) glacial snowpack where Hodson *et al.*,
104 (2017) provided evidence for differences detectable not only in the microbial community

105 composition, but also the biomass and nutrients of coastal and inland (glacial) snowpacks, thereby
106 highlighting changes over short distances (<1 km). A new study, carried out upon another maritime
107 Antarctic glacier (Signy Island), also revealed such differences between two coastal sites, as well
108 as within the vertical profile of a glacial snowpack with a substantial superimposed ice layer
109 (Hodson *et al.*, 2021). In this context, snowpack stratification and its effects on resident microbes
110 and nutrients could be significant. Therefore, this study will examine the ability of superimposed
111 ice to form a unique habitat or niche for microbial life.
112

113 To date, carbon balance studies in snowpacks lag behind studies in other glacial habitats, especially
114 cryoconite holes, supraglacial streams and lakes (e.g., Cook *et al.*, 2012; Dubnick *et al.*, 2017).
115 This is in spite of snowpacks being a recognised organic carbon reservoir (Priscu *et al.*, 2008) with
116 the ability to influence air-snow exchange processes (Amoroso *et al.*, 2010), downstream
117 ecosystems (Hood *et al.*, 2015) and the carbon cycle (Wadham *et al.*, 2019). Even fewer attempts
118 have been made to integrate carbon into an ecosystem model that can help us understand the
119 sources, sinks and transformations, and these have focused upon either surface glacial ice or
120 cryoconite (e.g., Hodson *et al.*, 2010; Cook *et al.*, 2012; Stibal, Bradley and Box, 2017). In this
121 study, biomass carbon will therefore be estimated, and its application to the quantification of
122 autotrophic and heterotrophic microbial production duly considered.
123

124 We therefore present the first comprehensive study of the microbial activity and biogeochemistry
125 of a melting snowpack on a High Arctic ice cap, Foxfonna. In so doing, we characterise seasonal
126 changes in microbial abundance, nutrient and chlorophyll concentrations within snow,
127 superimposed ice and glacial ice. Once the seasonal ecology of a melting snowpack on Foxfonna
128 has been established, autotrophic and bacterial production rates are investigated by estimating
129 cellular biomass change.
130

2 Materials and Methods

2.1 Study site

132 Foxfonna ($78^{\circ}07' - 78^{\circ}09' \text{N}$; $16^{\circ}06' - 16^{\circ}11' \text{E}$) is a small (4 km^2) mountain ice cap in Central
133 Spitsbergen, Svalbard (Figure 1), 2.31 km in diameter with elevations mainly between 550 and
134 808 m.a.s.l. (Kozioł 2014). Ground-penetrating radar surveys on Foxfonna show glacial ice that is
135 less than 80 m thick (Murray, T., Unpublished Data in Rutter *et al.*, 2011). These surveys suggested
136 that the ice cap is cold-based, as was established following the measurement of negative
137 temperatures in boreholes beneath its North Outlet (Liestøl, 1993).

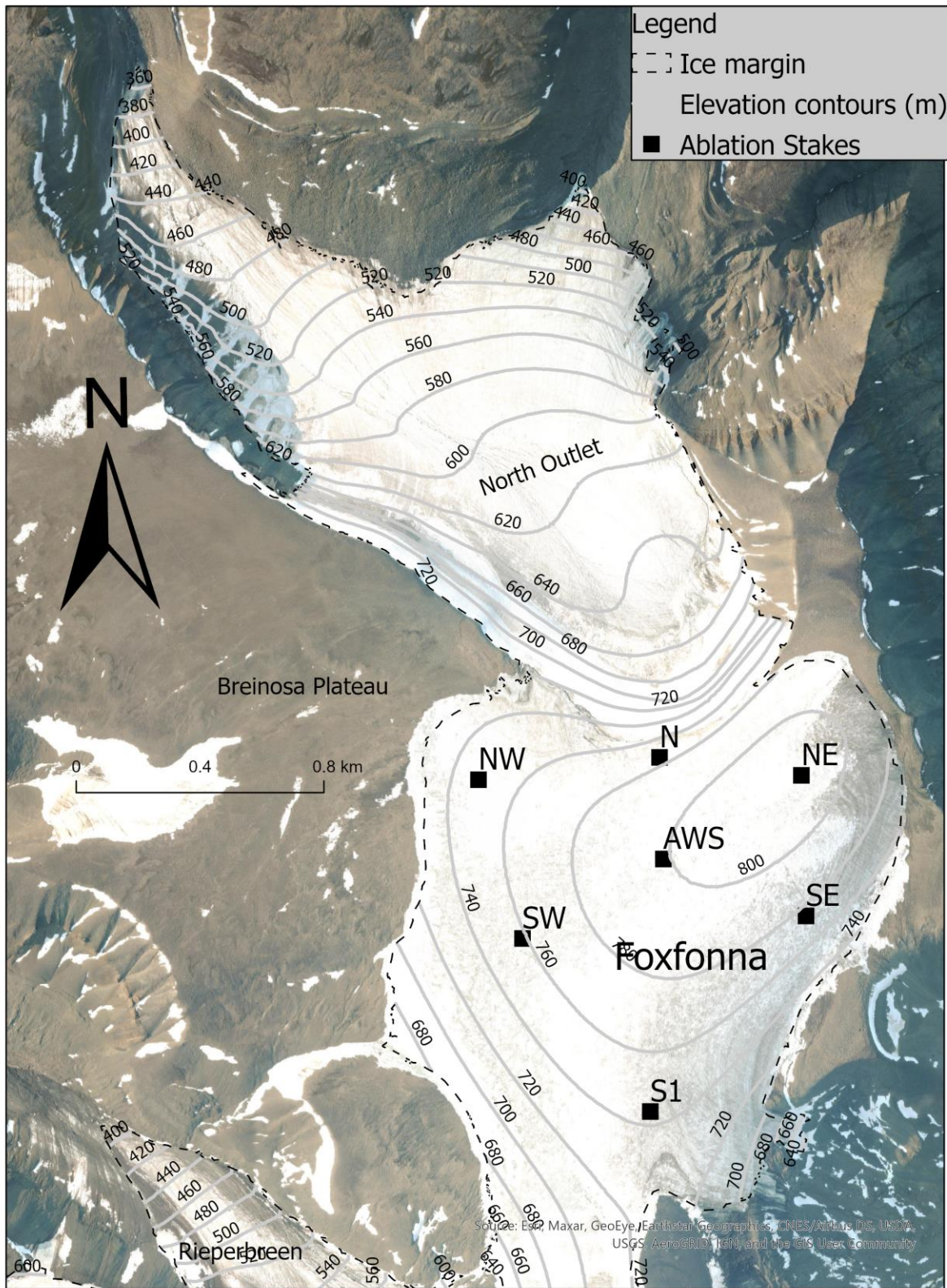


Figure 1. Foxfonna ice cap on Svalbard with ice margins and sampling sites marked.

139 **2.2 Snow pit sampling**

140 Figure 2 presents the key changes in snow depth and thermal conditions observed during the melt
141 season at Foxfonna, from April (pre-melt) to late July. In April, the snowpack was dry and cold
142 with a depth of ~1.5 m (at most sites). In addition, a layer of metamorphosed snow developed
143 between the glacial ice and the overlying snowpack due to vapour and temperature gradients during
144 the cold period.

145 A key transition period (hereafter “T1”) involved the development of a wet and larger, coarse-
146 grained snow surface as energy became available in response to the onset of summer, during June.
147 Although some minor melting occurred at the surface, snow temperatures remained below freezing
148 beneath it. The second important transition period, “T2”, from June to early July, was marked by
149 increasing temperatures, enhanced snowmelt and meltwater percolation to the bottom of the snow,
150 where refreezing occurred. The growth and development of superimposed ice at the snow-glacier
151 interface occurred during this period (when ice lenses also formed within cold snow patches above
152 it). Collectively, these processes removed the “cold content” of the snowpack and brought the
153 entire column up to the melting point. Thereafter, the isothermal melting snowpack slowly melted,
154 forming slush or basal meltwater and runoff, before exposing the underlying layer of superimposed
155 ice in July (transition period “T3”). Loss of this exposed superimposed ice as runoff occurred by
156 late July. Typically, a slushy mix of larger coarse-grained snow crystals, residual superimposed
157 ice and glacial ice was observed by this time, and glacier surface debris (cryoconite) became
158 obvious.

159
160 Field campaigns were therefore undertaken in 2016 for the purpose of a pre-melt survey (April)
161 and to coincide with transition periods: T1 in June, T2 in early July and T3 in late July (see Figure
162 2). Based on the directional aspect of Foxfonna, seven stakes (NW, SW, S1, AWS, SE, NE and N)
163 were chosen for snow pit sampling (Figure 1). At each of the seven stakes, the following samples
164 were collected into sterile Whirl-pak (*Nasco*) bags: surface snow (0 – 20 cm depth), mid snow
165 (from 20 cm depth to the base of the snowpack), superimposed basal ice and the underlying glacier
166 ice. These samples are hereafter referred to respectively as “TOP, MID, SUP ICE and GL ICE”.
167 Samples in April and June were collected using a pre-cleaned 8.5 cm diameter Federal Snow
168 Sampling Tube (Ricky Hydrological Co.). In July, the presence of slush and thick superimposed
169 ice required the use of a KOVACS Mark V ice corer (14 cm inner diameter) along with snow pit
170 sampling. A consistent core length of 25 cm GL ICE was extracted at each stake (Figure 1) during
171 the early and late July surveys only.

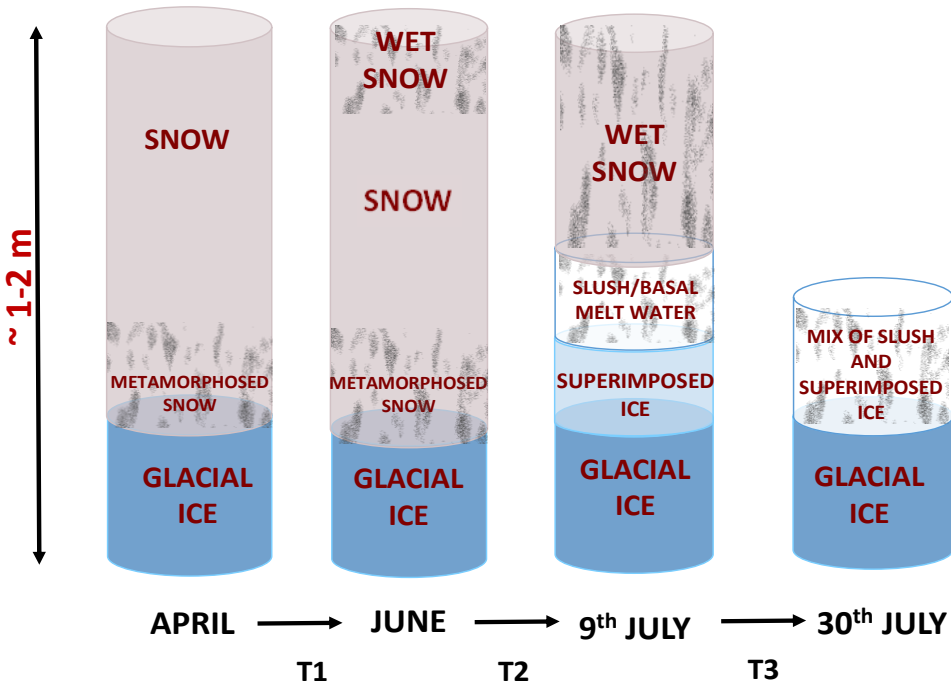


Figure 2. A schematic diagram showing the change in Foxfonna snowpack profile observed as melt season progressed from April (pre-melt to late July, 2016). Transition periods marked as T1, T2, T3.

173

174 2.3 Biogeochemical parameters

175 Samples were stored frozen in sterile 1L Whirl-paks (*Nasco*) at -20°C until their pre-processing at
 176 the University Centre in Svalbard (UNIS). To minimise biogeochemical changes, all the samples
 177 were melted in the dark at ambient room temperature. Powder-free nitrile gloves were used to
 178 handle all samples.

179

180 After thaw, samples were agitated and a 10 mL aliquot was immediately removed for a UV-based
 181 chlorophyll *a* fluorescence measurement. This was done using a Chelsea Unilux fluorimeter with
 182 a notional detection limit of 0.01 µg L⁻¹ and the average of 3 fluorescence readings were taken. pH
 183 measurements were conducted using a standard, portable meter and electrodes (Hanna
 184 Instruments, UK) calibrated using new pH 4 and 7 buffers. For microscopy analysis, 13 mL of
 185 subsample was removed using a sterile syringe, fixed with 1 mL of 0.2 µm-filtered 1% formalin
 186 and stored in sterile 15 mL Corning centrifuge tubes. The samples for microscopy were stored in
 187 the dark at 4°C until further analysis at the University of Sheffield, UK.

188

189 Analysis of other biogeochemical parameters such as nutrients and cell pigments required
 190 filtration. For nutrient analysis, 25- mL aliquots were filtered through 0.45 µm Whatman glass
 191 fibre filter paper (47 mm) using a glass filtration apparatus (acid-washed with 10% HCl). Filtered
 192 samples were stored in sterile 50 mL conical centrifuge tubes (VWR). Concentrations of cations
 193 Na⁺, K⁺, Mg²⁺, Ca²⁺ and anions Cl⁻, F⁻ and SO₄²⁻ were determined using the Dionex ICS90 ion

194 chromatography, calibrated in the range 0.01-1 mg L⁻¹ for cations and in the range 0.25-1 mg L⁻¹
195 for anions. The precision errors for these ions ranged from 0.9% to 1.6%, while the detection limit
196 was ≤ 0.05 mg L⁻¹ (calculated as three times the standard deviation of ten blanks). Quantification
197 of NH₄⁺, PO₄³⁻, NO₃⁻ and Si in the samples were conducted using a Skalar San++ Continuous Flow
198 Analyser, calibrated in the range 0-3 mg L⁻¹. The limit of detection for these ions was ≤ 0.05 mg
199 L⁻¹ (calculated as three times the standard deviation of ten blanks), while the limit of quantification
200 was ≤ 0.2 mg L⁻¹. These analyses employed standard colorimetric methods (based on The
201 European Standard EN ISO, 1996, 2002, 2004 and 2005). Data for other ions analysed such as
202 Na⁺, K⁺, Mg²⁺, Ca²⁺, F⁻, SO₄²⁻, Si and DOC are not shown (see Supplementary Tables S1 – S4)
203 and are only discussed in the context of factor analysis of the entire data set (Section 3.2).

204

205 **2.4 Pigment concentration**

206 Melted samples (up to 420 mL) were filtered onto 0.45 µm Whatman glass fibre filter paper (47
207 mm). Filters were individually wrapped in aluminium foil and returned frozen to the UK for
208 analysis. Further, frozen filter papers were transported insulated with reusable refrigerant polar gel
209 packs (ThermoSafe®) in a polystyrene box to the University of Bristol and immediately stored at
210 -80°C. Filters were then freeze-dried (for 24 hours), and High-Performance Liquid
211 Chromatography (HPLC) analysis of the samples was undertaken following procedures described
212 in Williamson *et al.* (2018, 2020).

213

214 **2.5 Epifluorescence microscopy for cell counts**

215 The glass filtration set-up was rinsed and cleaned with 70% ethanol prior to analysis and in-
216 between samples to avoid contamination. Ten mL of sample was filtered through a 0.2 µm Poretics
217 Polycarbonate Track Etched Black (25 mm, *Life Sciences*) filter paper, processed, followed by the
218 addition of a combination of SYBR Green II (*Molecular Probes*) and Propidium Iodide (PI,
219 *Invitrogen*) stains. The stain combination comprised of 10 µL of SYBR Green II (1x working
220 solution) and 5 µL of 1.5 mM PI prepared in 1 mL of Dimethyl Sulfoxide (DMSO) solution. The
221 dual stained sample was allowed to incubate for 15 minutes in the dark and was then filtered. This
222 dual-stained approach was developed from flow cytometric viability studies on freshwater and
223 marine bacteria (Lebaron, Parthuisot and Catala, 1988; Barbesti *et al.*, 2000; Grégoire *et al.*, 2001)
224 as well as live/dead cell counts of bacteria in drinking water (Sysmex, Partec). The filter paper was
225 then placed onto a glass slide, a drop of SlowFade® Diamond Antifade Mountant added to it, excess
226 fluid removed and then covered with a coverslip, ready for imaging.

227

228 For bacterial cell counts, a Widefield Nikon Live-Cell System was used at 100x magnification,
229 and microscopic fields were captured to count a minimum of 300 cells (Cook *et al.*, 2020), which
230 was not always possible (e.g. for clean snow samples). The stained samples were excited at 470
231 nm and detected via filter cubes. Autotrophic cell counts were undertaken at 20x, 40x and 63x and
232 viewed under UV (for chlorophyll *a* fluorescence) and bright-field.

233

234 After imaging, images were converted to 8-bit greyscale on the software ImageJ. Cells were
235 counted using the *Analyze Particles* function with a size range of 0.2 to 2 µm² and a circularity of
236 0 to 1. This was done to exclude the counting of mineral debris and remove noise. Filamentous
237 bacteria or snow algae were measured manually on the software, as they were larger (10 – 20 µm).
238 The cell counts (cells mL⁻¹) were calculated as a product of the counts per image and the
239 microscope's field of view (FOV), divided by the volume of the sample filtered.

240 **3 Results**

241

242 **3.1 Seasonal change in snow cover, nutrients, cells and chlorophyll on Foxfonna**

243 The glacier mass balance conditions that were experienced during the study included the joint
244 highest (i.e., 54 cm w.e.) winter snow accumulation since records began in 2007. The summer
245 ablation was the fourth highest for the same interval (average-119 cm w.e.), causing a near-
246 complete disappearance of the snowpack during the summer that is rather typical of this site. Figure
247 3A shows the evolution of the average snow water equivalent (SWE) through the melt season.
248 Average values for the seven stakes ranged from 53 - 56 cm water equivalent (w.e.) from April
249 until early July, and then dropped to 8 cm w.e. by the end of July (including any residual
250 superimposed ice): most of which was near Stake N. Growth of superimposed ice commenced
251 during T2 (June to early July) and formed an average water equivalent of 11 ± 5.4 cm w.e. (not
252 shown). Depletion of combined snow and superimposed ice to 1 ± 2.5 cm w.e. occurred during
253 transition period T3 (early to late July), according to the late July survey. In late July, the high
254 standard deviation was due to superimposed ice being left at only one stake (AWS).

255

256 Nutrient loading at each stake was calculated from the product of the SWE (cm w.e.) of separate
257 TOP, MID and SUP ICE samples and their corresponding nutrient concentration (mg L^{-1}), which
258 were then summed to produce the total mass (or “loading”) at each stake location in mg m^{-2} .
259 Averages of these nutrient loading values at the stakes were then estimated for each survey to
260 reveal seasonal changes across the entire ice cap. Comparison between SWE and Cl^- loadings
261 (Figure 3 A and B) show leaching of Cl^- from the snowpack between June and early July (i.e.
262 transition period T2), because the Cl^- loading decreased more rapidly than SWE. Average Cl^-
263 loadings for the entire ice cap stayed below 1000 mg m^{-2} with the lowest value observed at the end
264 of July: $53 \pm 85 \text{ mg m}^{-2}$. By comparison, loadings of NH_4^+ and PO_4^{3-} were as much as two orders
265 of magnitude lower, as is expected in such an oligotrophic environment. NH_4^+ ranged from $1 - 22$
266 mg m^{-2} and PO_4^{3-} ranged even lower, at $0.4 - 13.9 \text{ mg m}^{-2}$ through the melt season. Interestingly,
267 during T2 (June – early July), NH_4^+ and PO_4^{3-} loadings increased whilst Cl^- and NO_3^- decreased.
268 In fact, NH_4^+ and PO_4^{3-} loadings reached their highest values sometime after the onset of significant
269 melting during early July at 22 and 13.9 mg m^{-2} , respectively. Surprisingly, NO_3^- did not show its
270 highest loading at the same time as NH_4^+ . Instead, NO_3^- was leached rather like Cl^- and ranged
271 from $0.5 - 15.4 \text{ mg m}^{-2}$.

272

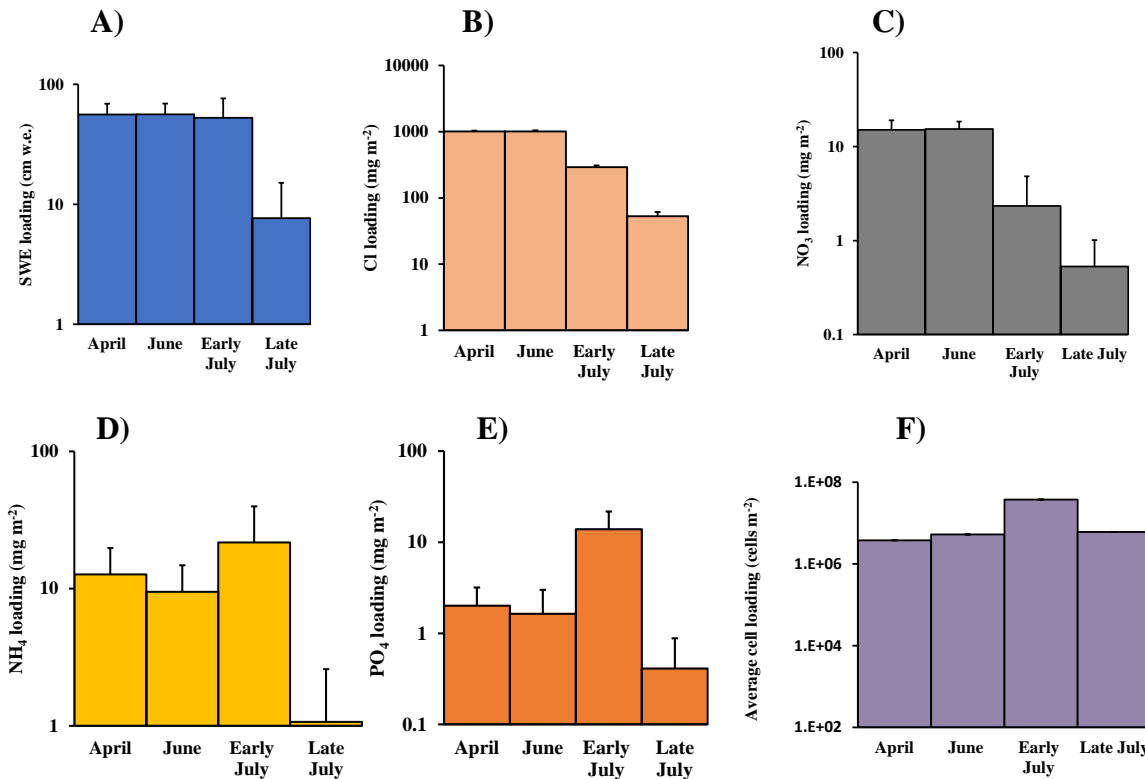


Figure 3. Seasonal change in Snow Water Equivalent (SWE), average loadings (mg m^{-2}) for Cl^- , NO_3^- , NH_4^+ , PO_4^{3-} and cell loading on Foxfonna ice cap. Error bars are standard deviations ($n=7$)

273
274
275
276
277
278
279
280
281

Bacterial cell loading (cells m^{-2}) at each stake was calculated in an identical manner to the nutrient loading estimates (Figure 3F). Seasonal variations in the average cell loading across Foxfonna revealed minimal change during transition period T1, a significant increase ($p\text{-value} = 0.05$ where $\alpha = 0.05$) from $5.3 \times 10^6 (\pm 2.7 \times 10^5)$ to $3.8 \times 10^7 (\pm 4.3 \times 10^6)$ cells m^{-2} occurred during transition period T2 (June to early July). A decrease to $6.1 \times 10^6 (\pm 1.6 \times 10^6)$ cells m^{-2} followed during T3 (early to late July), although this was insignificant at the 95% confidence level ($p\text{-value} = 0.3$ where $\alpha = 0.05$), due to strong spatial variability in cell concentrations.

282
283
284
285
286
287
288
289
290
291
292

Chlorophyll *a* was the dominant pigment within snow, superimposed ice and glacial ice (Supplementary Figure S2). The Unilux derived chlorophyll *a* concentration within snow, superimposed ice and glacier ice ranged between 1.7 and $13 \mu\text{g L}^{-1}$ (Supplementary Figure S3). There was no significant change within the TOP and MID snows during transition periods T1 and T2, i.e., between April and June, where it lay in the range $1.7 - 2.7 \mu\text{g L}^{-1}$ and from June to early July, $1.7 - 1.9 \mu\text{g L}^{-1}$. GL ICE displayed the highest chlorophyll *a* concentration at $13 \mu\text{g L}^{-1}$ and $10.7 \mu\text{g L}^{-1}$ in early and late July, respectively. However, when the snow samples were examined under the microscope, no autotrophic cells were detected in most samples. A slight increase in the cell numbers, e.g., to 25 cells mL^{-1} , yielded chlorophyll *a* concentration of $3 \mu\text{g L}^{-1}$. Therefore, a comparison between the Unilux-measured (in-vivo fluorescence) chlorophyll *a* and HPLC-derived extracted chlorophyll *a* concentrations was undertaken using bulk samples. This yielded a

293 moderate correlation ($r = 0.77$, $p < 0.05$) with a significant intercept of $2.1 \mu\text{g L}^{-1}$, indicating the
294 presence of a non-biological signal affecting the Unilux sensor (Supplementary Figure S4).
295 Furthermore, the “background” Unilux measurements for samples with no detectable autotrophs
296 (according to microscopy) was almost always $2 \mu\text{g L}^{-1}$. Therefore, it is highly likely that another
297 source of fluorescence – such as mineral autofluorescence – is present in the signal, and so the
298 Unilux readings cannot be used to say that autotrophs were present.
299
300

301 **3.2 Factor Analysis**

302 Factor analysis was undertaken to establish the sources and differential behaviour of the nutrients,
303 cells and chlorophyll. All major ion analyses were included in the analyses. To preserve the
304 variance in the entire dataset, all the separate TOP, MID and SUP ICE samples were used, rather
305 than combined values for each stake. The statistical package SPSS identified six factors with Eigen
306 Values > 1 , which collectively explained 76% of the total variance in the dataset. However, only
307 the first three factors produced strong loadings (> 0.7) and were thus amenable to interpretation.
308 Table 1 shows these three factors, highlighting the variables with either strong or moderate
309 loadings (between 0.4 and 0.69) in each case. The first Factor (F1) showed strong positive loadings
310 in the order Na^+ , Mg^{2+} , Cl^- , Ca^{2+} , SO_4^{2-} and NO_3^- . There were also strong or moderate negative
311 loadings from PO_4^{3-} and Si. At first glance, Factor 1 seems to be dominated by marine aerosol.
312 However, ratios of Ca^{2+} to Cl^- (both being strong contributors to Factor 1) were in excess of
313 standard marine water ratios, showing a significant non-sea-salt supply of Ca^{2+} (average 85%: data
314 not shown). Therefore, Factor 1 most likely reflects the leaching (elution) of solute from the
315 snowpack, which is dominated by (but is not exclusive to) solute derived from marine aerosol. The
316 strong or moderate negative loadings of PO_4^{3-} and Si respectively were unexpected, but might
317 indicate a different source that became more apparent as the elution of mobile ions progressed.
318 The second Factor (F2) explained 16% of the variance in the dataset, and was dominated by
319 moderate to strong loadings for DOC, total cell abundance and chlorophyll *a* (0.61, 0.72 and 0.69).
320 It is tempting to suggest that photosynthetic microbes such as cyanobacteria might be responsible
321 for the presence of all three of these variables, but no significant loading was observed with the
322 autotrophic cell abundance due to their absence in the snow. Instead, it seems more likely that
323 Factor 2 represents similar behaviour of bacterial cells, DOC and small, autofluorescent mineral
324 particles that perhaps cause variations in the background chlorophyll *a* readings. Therefore Factor
325 2 most likely reflects the mobility of particles in the snow matrix during the summer and their
326 provision of NH_4^+ .
327

328 Like Ca^{2+} , K^+ showed a strong non-marine contribution (average 91%), yet it loaded strongly onto
329 F3 along with NH_4^+ (0.76 and 0.73, respectively). This is most likely indicative of dust or clay
330 weathering processes, as NH_4^+ and K^+ act as interchangeable cations in clay-mineral lattices, and
331 are easily extractable following adsorption onto dust or clay particles.
332

Table 1. Factor loading analysis for all samples through the melt season. Moderate loadings (i.e., between 0.4 and 0.69) and strong loadings (i.e., > 0.7) are marked by “*” and “**” respectively.

Parameter	Factor 1	Factor 2	Factor 3
Na ⁺	0.794**	-0.090	0.074
K ⁺	0.004	-0.113	0.758**
Mg ²⁺	0.778**	0.265	0.158
Ca ²⁺	0.688**	0.496*	0.228
F ⁻	0.293	0.081	-0.041
Cl ⁻	0.769**	-0.286	0.189
NO ₃ ⁻	0.610**	-0.473*	-0.211
NH ₄	-0.268	-0.277	0.727**
PO ₄ ³⁻	-0.743**	0.111	0.354
SO ₄ ²⁻	0.650**	-0.205	-0.108
Si	-0.648**	0.012	0.254
Chlorophyll <i>a</i> (Chl)	0.235	0.695**	0.320
Autotrophic cell abundance	0.094	0.213	-0.165
Total cell abundance	-0.200	0.718**	-0.277
Dissolved Organic Carbon (DOC)	0.433*	0.606**	0.403*

333 3.3 Seasonal bacterial production on Foxfonna

334 Bacterial cell loading estimates (Figure 3F) were used to estimate the total bacterial biomass on
 335 Foxfonna, such that the bacterial production (BP) could be estimated from rate of change in
 336 biomass (BM) per unit time. Bacterial production was assumed to be negligible during period T1
 337 on account of there being very little liquid water in the cold snowpack (see Figure 2). Therefore,
 338 period T2 was the most suitable period for applying this approach, because changes in cell loading
 339 were likely dominated by bacterial production on account of the high-water content and its
 340 capillary retention within the snow (Reijmer *et al.*, 2012). The loss or gain of bacterial cells by
 341 wind-blown snow transport is also likely to have been suppressed greatly by the high-water content
 342 in the older snow, and the lack of fresh snowfall events (hence the negligible change in total SWE
 343 during T2 on the ice cap shown in Figure 3A).

344
 345 Under the assumption that only bacterial growth dominated the bacterial cell loading change
 346 during transition period T2, bacterial production in snow and superimposed was estimated thus:

$$BP_{\text{snow}\pm\text{SI}}^{T2} = c \cdot \left(\frac{\overline{BM}_{\text{snow}}^{\text{early july}} - \overline{BM}_{\text{snow}}^{\text{june}} + \overline{BM}_{\text{SI}}^{\text{early july}}}{T2} \right) \quad (1)$$

Where $BP_{\text{snow}\pm\text{SI}}^{T2}$ is the combined average daily bacterial production during T2 for snow and superimposed ice ($\text{mg C m}^{-2} \text{ d}^{-1}$), T2 is the transition period duration i.e., 32 days, \overline{BM} is average biomass, estimated from average snow or superimposed ice (SI) cell loading on the ice cap (cells m^{-2}). Note that since no superimposed ice layer existed in June, only its cell content in the early July survey needed to be included in the census. Finally, c = carbon content of each cell according to Takacs and Priscu (1998).

353

The results suggest transition period T2 was marked by an increase in bacterial biomass by an order of magnitude throughout the entire snow/ice layer of $2.4 \pm 1.5 \times 10^{-5} \text{ mg C m}^{-2} \text{ d}^{-1}$. Of this, up to $1.0 \pm 0.5 \times 10^{-5} \text{ mg C m}^{-2} \text{ d}^{-1}$ was stored in SUP ICE (the rest being bacterial cells already present in the snow at the onset of T2). Furthermore, biological production cannot be separated between snow and superimposed ice, because all of the bacteria in the ice could have been washed downwards whilst the superimposed ice was forming.

360

Although conditions were similar during T3, this transition period was dominated by runoff, as shown by the marked SWE depletion in Figure 2. Therefore, it is important to take into account the loss of cells with this runoff, as indicated below. However, it must be noted that cells lost during runoff are more likely to be bacterial than autotrophic, due to the latter's propensity to form cryoconite aggregates and persist for several years on the glacial surface (Hodson, Cameron, *et al.*, 2010).

367

$$BP_{\text{snow}\pm\text{SI}}^{T3} = c \cdot \left(\frac{\overline{BM}_{\text{snow}}^{\text{late july}} - \overline{BM}_{\text{snow}}^{\text{early july}} + \overline{BM}_{\text{SI}}^{\text{late july}} - \overline{BM}_{\text{SI}}^{\text{early july}} + RU_{\text{cells}}^{T3}}{T3} \right) \quad (2)$$

Where RU_{cells}^{T3} is the runoff flux of cells normalised for ice cap area (i.e., cells m^{-2}) and T3 is the duration of Transition period 3, i.e., 23 days. However, uncertainty in RU_{cells} is such that biological production could not be estimated directly during this period. Daily rates of bacterial production in the snowpack and the superimposed ice during T3 were therefore assumed to be half of that deduced from T2, to account for the depletion of SWE to almost zero during this interval.

373

The rates of seasonal bacterial production were therefore estimated to be negligible in transition period T1 (due to low free water content within the snow), to be $2.4 \pm 1.5 \times 10^{-5} \text{ mg C m}^{-2} \text{ d}^{-1}$ during transition period T2 and to be $1.2 \pm 0.75 \text{ mg C m}^{-2} \text{ d}^{-1}$ during transition period T3. The near-complete ablation of the snowpack and superimposed ice after this means their contribution to bacterial production would have been negligible, and the ecosystem dominated by biological production upon the glacier surface. The total bacterial production within the snow and superimposed ice for the combined 55 days of T2 and T3 was therefore $153 \text{ mg C m}^{-2} \text{ a}^{-1}$.

381

382 **3.4 Spatial variations in nutrient concentrations and cells**

383 “TOP” and “MID” snow samples were compared with the superimposed ice and glacial ice
 384 samples (“SUP ICE” and “GL ICE”, respectively) with respect to the essential macronutrients
 385 NH_4^+ and PO_4^{3-} , due to the unexpected increase in their concentrations revealed by Figure 3 D and
 386 E. We found that average NH_4^+ concentrations ranged from 0 to 0.04 mg L^{-1} in the April samples
 387 of TOP and MID snow (Supplementary Figure S1). However, after the onset of melt and
 388 superimposed ice formation, greater average NH_4^+ concentrations ($0.05 \pm 0.05 \text{ mg L}^{-1}$) appeared
 389 in SUP ICE than in the TOP and MID snows (0.03 ± 0.01 and $0.04 \pm 0.03 \text{ mg L}^{-1}$, respectively).
 390 Concentrations in GL ICE were higher still, but more variable (average $0.07 \pm 0.1 \text{ mg L}^{-1}$ in early
 391 July). The variability was caused by high values at Stake SE (Data Not Shown): a site notable for
 392 a high concentration of surface debris. Average PO_4^{3-} concentrations were an order of magnitude
 393 lower than NH_4^+ in April and June i.e., from 0.003 to 0.005 mg L^{-1} in TOP and MID snows
 394 (Supplementary Figure S1). No PO_4^{3-} was detected in the top layer at stake S1. However, these
 395 concentrations increased in early July and ranged from 0.02 - 0.03 mg L^{-1} in TOP and MID snows.
 396 SUP ICE exhibited similar concentrations (average $0.03 \pm 0.007 \text{ mg L}^{-1}$).
 397

398 Table 2 shows autotrophic (snow algae and cyanobacteria) and bacterial concentrations (in cells
 399 mL^{-1}) identified through bright-field and epifluorescence microscopy. Average cells mL^{-1} are
 400 given for all snow (TOP and MID combined), SUP ICE and GL ICE. The average autotrophic cell
 401 abundance on the ice cap through the melt season was $0.5 \pm 2.7 \text{ cells mL}^{-1}$. The large standard
 402 deviation throughout the dataset indicates high spatial variability. All the autotrophic cells in April
 403 snow were identified as cyanobacteria, of which 68% were found on the southern and uppermost
 404 part of the ice cap (Stakes S1, SW and AWS). Surprisingly, no significant numbers of autotrophic
 405 cells were identified in snow for June, early July or late July. No significant numbers of autotrophic
 406 cells were observed in superimposed ice either. The only changes in average autotrophic cell
 407 abundance were identified from early to late July due to increases in cyanobacteria (e.g., 0.1 ± 0.4
 408 to $2 \pm 4 \text{ cells mL}^{-1}$ in GL ICE) and also snow algae (e.g., 0.04 ± 0.1 to $0.3 \pm 0.5 \text{ cells mL}^{-1}$ in SUP
 409 ICE). However, snow algal cells were so few and dispersed that their average number on the ice
 410 cap often resulted in an unusable value ($\sim 0 \text{ cells mL}^{-1}$). By contrast, the average bacterial
 411 abundance on the ice cap was far greater and increased by an order of magnitude from ca. 10^2 cell
 412 mL^{-1} to almost $10^3 \text{ cells mL}^{-1}$. Table 2 shows that changes in the bacterial cell abundance of SUP
 413 ICE and GL ICE were more muted than changes in the total snowpack bacterial cell abundance. It
 414 also shows that both bacteria and autotrophic cell abundance decreased between April and June.
 415 However, the decrease is an artefact of two highly concentrated samples at Stake N that were
 416 encountered in April (data not shown). Spatial variability is therefore a major characteristic of the
 417 cell distribution across the ice cap, and we could discern no clear patterns underlying this
 418 variability, either from stake to stake, or amongst the different sample types.
 419
 420
 421
 422
 423
 424
 425
 426
 427

428
429Table 2. Average cell abundance on Foxfonna. Values are average \pm standard deviation.

Sample type	Month	Snow algae (cells mL ⁻¹)	Cyanobacteria (cells mL ⁻¹)	Bacteria (cells mL ⁻¹)
All Snow	April	0	5 \pm 9	81 \pm 124
	June	0	0	39 \pm 19
	Early July	0.2 \pm 0.4	0	363 \pm 595
	Late July	0.1 \pm 0.3	0.7 \pm 1.5	935 \pm 1460
SUP	Early July	0.04 \pm 0.1	0	299 \pm 306
ICE	Late July	0.3 \pm 0.5	0.1 \pm 0.4	185 \pm 0
GL ICE	Early July	0.5 \pm 0.7	0.1 \pm 0.4	565 \pm 575
	Late July	0.3 \pm 0.6	2 \pm 4	818 \pm 792

430 **4 Discussion**

431

432 **4.1 Nutrient sources and their non-conservative behaviour in the snowpack**

433 Despite being largely associated with long-range atmospheric pollution (Kühnel *et al.*, 2013), NO₃⁻
 434 showed a strong, positive loading onto Factor 1 that was similar to that of Cl⁻, a biogeochemically
 435 conservative ion associated with marine aerosol. Therefore, NO₃⁻ co-eluted with Cl⁻ and seems to
 436 have been largely conservative during meltwater export (e.g. Tranter and Jones, 2001). By
 437 contrast, Figure 3 shows that, NH₄⁺ and PO₄³⁻ demonstrated a marked increase in abundance during
 438 July, resulting in either a negative loading onto Factor 1 (PO₄³⁻) or loading onto the separate Factor
 439 3 (NH₄⁺). Thereafter, both NH₄⁺ and PO₄³⁻ demonstrated an equally marked decrease during July
 440 (period T3), which seems to be caused entirely by the rapid ablation of the snowpack. Since the
 441 initial, sharp increase in NH₄⁺ and PO₄³⁻ coincided with period T2, when liquid water availability
 442 rose markedly within the snow matrix, we invoke a dissolution process involving wind-deposited
 443 clay and dust particles as the cause.

444

445 Dust deposition onto Foxfonna is well known due to the exposure of the desiccated Adventdalen
 446 river bed prior to early summer inundation by meltwater (as well as afterwards in early winter).
 447 Therefore, it is likely local dust deposited at the surface (early summer) and the base (early winter)
 448 of the 2015/16 snowpack was available for dissolution. Interestingly, the apparent conservative
 449 behaviour of NO₃⁻ during the same period provided no evidence for oxidation of the NH₄⁺ to NO₃⁻
 450 , as has been proposed in dry winter snowpacks by Amoroso *et al.*, (2010). However, conversion
 451 of NH₄⁺ to NO₃⁻ is readily observed when snowmelt passes through environments that offer greater
 452 rock-water contact than the snowpack, such as those at the margins of glaciers (e.g. Hodson *et al.*,
 453 2010). NO₃⁻ therefore seems to demonstrate largely conservative behaviour when residence times
 454 are reduced following the onset of melting conditions during summer.

455

456 In summary, local dust-derived sources of NH₄⁺ and PO₄³⁻ appear to have combined with long
 457 range (marine and anthropogenic aerosol) sources responsible for NO₃⁻ to deliver critical macro-
 458 nutrients to the Foxfonna snowpack during 2015/16.

459

460 4.2 No utilization of nutrients by autotrophic communities

461 The present study demonstrated nutrient behaviour not shown by biologically active snowpacks
462 elsewhere, because the NH₄⁺ and PO₄³⁻ released by weathering processes during T2 were not
463 sequestered for autotrophic growth and activity. The acquisition of macronutrients such as NH₄⁺,
464 NO₃⁻ and PO₄³⁻ from rock debris and marine fauna in Antarctica are well known to stimulate
465 autotrophic growth in nutrient-limited snowpacks (Fujii et al., 2010; Hodson et al., 2017). For
466 example, in coastal snowpacks of Livingston Island, Antarctica, the removal of NH₄⁺ and PO₄³⁻
467 from the snow correlated with increasing chlorophyll *a* concentrations that were significantly
468 greater than those reported at Foxfonna. Therefore utilisation of these nutrients by the resident
469 autotrophic communities was a dominant feature of the Livingston Island data set (Hodson et al.,
470 2017b). By contrast, their removal by primary production is conspicuous by its absence in the
471 Foxfonna data.

472

473 Nutrients that have yet to be considered could have been responsible for limiting algal growth,
474 such as dissolved inorganic carbon or Fe (Hamilton and Havig, 2017). However, the local geology
475 of Adventdalen valley is dominated by sandstones, siltstones and shales (Rutter et al., 2011) –
476 whose dust deposition within the snow offers DIC and Fe from a range of minerals through natural
477 weathering processes (see Hodson et al., 2017a). Therefore, nutrient limitation seems to be an
478 unlikely explanation for the lack of autotrophic growth on Foxfonna during the study period.
479 Furthermore, a recent study did encounter a significant population of red snow algae and ice algae
480 in snow and ice samples on Foxfonna (Fiolka et al., 2021). This study was conducted in late August
481 in 2011, and suggests, in accordance with the authors' own observations throughout 15 years of
482 mass balance survey, that there is marked annual variability in snow algae population dynamics.
483

484

485 An important environmental factor is likely to have been the role that the heterogeneity of the
486 snowpack plays in governing how conducive it becomes for autotroph proliferation, especially
487 since a great many would be expected to reside on the glacier surface prior to the onset of snowmelt
488 (Stibal et al., 2015). For example, the nutrient resource available within the snowpack layers
489 (Figure 3) would have presented an excellent opportunity for flagellated vegetative forms of green
490 algal cells to make their way upwards towards the snow surface, seeking light and nutrients (Stibal
491 et al., 2007). However, their motility from the glacier surface through the snowpack was most
492 likely impeded by the refrozen superimposed ice layer and other ice lenses that formed during
493 transition period T2.

494

495 Given the above, the most important limitation to the autotrophic production seems to be
496 insufficient inocula of snow algal cells within the fresh winter snowpack (and potentially upon the
497 previous summer surface) to allow germination of new cells (Hoham et al., 2006). Therefore, it is
498 proposed that the sustained, low autotrophic cell abundance is most likely caused by the high
499 elevation of Foxfonna and its sustained negative mass balance, which is responsible for the
500 removal of all snow from the summit of the ice cap, leaving no residual firn to provide inocula to
501 meltwaters percolating down through the system. Secondly, the community typically has only a
502 short opportunity to respond to the increase in energy and nutrients during summer (55 days)
503 before biomass is removed by further ablation. Finally, since the environment under study is by
504 no means unique, the likely response of the snowpack autotrophic community in other high
505 elevation polar ice caps might also be restricted in this way, suggesting that many will be
dominated by bacterial production as they lose their perennial snow covers.

506
507

4.3 Assessing the importance of bacterial carbon production on Foxfonna

508 Significant changes in carbon resources were detectable during T2 because bacterial cell
 509 abundance increased from 39 ± 19 to 363 ± 595 cells mL^{-1} (Table 2). These bacterial cell numbers
 510 are more representative of Antarctic snows (Carpenter, Lin and Capone, 2000; Michaud et al.,
 511 2014) than the Arctic or Alpine snows (Amato et al., 2007) and were used to estimate bacterial
 512 production during transition periods T2 and T3 was ca. $153 \text{ mg C m}^{-2} \text{ a}^{-1}$ (Section 3.2). For these
 513 calculations, a fixed bacterial carbon content per cell ($11 \text{ fg C cell}^{-1}$) was employed based on prior
 514 work on carbon reservoirs in polar habitats (Kepner et al., 1998; Takacs and Priscu, 1998; Priscu
 515 et al., 2008). This value of $11 \text{ fg C cell}^{-1}$ had been previously used: 1) to calculate carbon released
 516 from microbial populations via viral lysis in Antarctic lakes (Kepner, Wharton and Suttle, 1998),
 517 2) to understand the bacterioplankton dynamics in permanently ice-covered lakes in the McMurdo
 518 Dry Valleys, Antarctica (Takacs and Priscu, 1998), and most importantly, 3) to estimate
 519 prokaryotic cellular carbon reservoir in all Antarctic habitats, namely, lakes, subglacial aquifers
 520 and the ice sheets (Priscu et al., 2008). These estimates, although published in 2008, did not use
 521 any of the available allometric and linear volume-to-carbon conversion factors. These factors,
 522 compiled by Posch et al. (2001), were, however used by Bellas et al. (2013) to estimate a range for
 523 bacterial carbon production in Arctic cryoconite sediments.

524

525 Irvine-Fynn et al. (2012) quantified cell budgets on an Arctic glacier surface using flow cytometry,
 526 compared both cell-to-carbon and volume-to-carbon conversions, but opted for the higher value
 527 of $20 \text{ fg C cell}^{-1}$ (from Whitman, Coleman and Wiebe, 1998), to estimate annual carbon export
 528 from a supraglacial catchment on Midtre Lovénbreen (Svalbard). In their study, the cell
 529 abundance, size and shape were enumerated through flow cytometry, classified on the basis of
 530 size. With the greatest proportion of cells being $\leq 3 \mu\text{m}$, they were presumed to be spherical-shaped
 531 heterotrophic bacteria. It is also interesting to note that the value of $20 \text{ fg C cell}^{-1}$ applied for
 532 heterotrophic cell carbon production by these authors, has also been used to estimate autotrophic
 533 snow algal carbon production in several Arctic/Antarctic carbon estimation studies (e.g. Fogg,
 534 1967; Takeuchi et al., 2006). On the other hand, for their allometric volume-to-carbon estimation,
 535 wherein spherical shaped cells were assumed, the formula given by Felip et al. (2007) was applied:

$$CC = 120 \times V^{0.72} \quad (3)$$

536
537

Where CC is the carbon content (fg C cell^{-1}) and V is the biovolume (μm^3).

538
539
540
541
542
543
544
545
546

This formula, however, was used for rod-shaped bacteria to study bacterial biomass in mountain
 lakes (Felip et al., 2007), and earlier to estimate biomass in the snow and ice covers of such lakes
 (Felip et al., 1995). This allometric model was originally given by Norland et al. (1993), where the
 geometric shape of the bacteria was approximated as a cylinder with hemispherical ends, based on
 electron microscopy and X-ray analysis of bacterial cultures. It is unclear whether the carbon
 content formula stays relevant for spherical bacterial cells or was intended to be used only for rod-
 shaped cells. This shows that differences in methods for volume estimation and the carbon content,
 can introduce significant variability in the carbon budget estimations and therefore the need arises
 to have a consensus and a standard on the parameters that are to be used for such estimations.

547
548
549
550
551

The summary of conversion factors from (Posch et al., 2001) incorporates different size range, habitat, preparation techniques and growth conditions, but would have benefited from inclusion of a column listing the method for volume estimation involved in each of the referenced methods. Therefore, the worker needs to be careful and take into account the different parameters being used

Table 3. Cell-to-carbon and volume-to-carbon bacterial carbon production values during T2 (June – early July) on Foxfonna.

Sampling Survey (Transition period)	Estimated areal bacterial production (mg C m ⁻² day ⁻¹) in snow
Cell-to-carbon	[*] 2.4 x 10 ⁻⁵ ± 4 x 10 ⁻⁵
	['] 4.3 x 10 ⁻⁵ ± 7.3 x 10 ⁻⁵
Allometric C-per-cell	[~] 1.2 ± 2
	['] 1.9 ± 3.2

Note: Cellular carbon content ^{*}11 fg C cell⁻¹ (Takacs and Priscu, 1998), [']20 fg C cell⁻¹ (Whitman, Coleman and Wiebe, 1998), [~] assumes allometric C-per-cell from ^{*}(Felip et al., 2007) and ['](Posch et al., 2001)

552 during selection of the appropriate model for their use. It might not be possible to reach a
553 worldwide consensus on carbon estimation protocols yet, but it is important that a laboratory group
554 produce repeatable estimations following a standard protocol so that they may be comparable and
555 significant errors can be avoided.
556557 For comparison purposes, Table 4 compiles bacterial carbon production numbers on a daily basis
558 for all cell-to-carbon and volume-to-carbon conversions calculations discussed above. For obvious
559 reasons, using 20 fg C cell⁻¹ instead of 11 fg C cell⁻¹ results in a bacterial carbon production value
560 which is nearly double (e.g., for snow: 2.4 x 10⁻⁵ ± 4 x 10⁻⁵ mg C m⁻² day⁻¹ and 4.3 x 10⁻⁵ ± 7.3 x
561 10⁻⁵ mg C m⁻² day⁻¹). In contrast, the cell-to-volume allometric conversions are ~ 5 orders of
562 magnitude higher (1.2 ± 2 mg C m⁻² day⁻¹ and 1.9 ± 3.2 mg C m⁻² day⁻¹). This shows that the use
563 of these two different approaches can introduce significant uncertainty in the carbon budget and
564 there needs to be both a standardisation of techniques and a consensus as to which conversion
565 approach should be employed. The range of results here makes comparison with other studies
566 difficult. For example, the bacterial carbon production values for two glacial snowpacks in the
567 maritime Antarctic (Signy island) that were deduced using radiolabel incorporation experiments
568 were significantly higher than in this study (11 ± 12 and 17 ± 11 mg C m⁻² d⁻¹), but the difference
569 can to some extent be attributed to the higher bacterial cell abundance at Signy (10³ - 10⁴ cells mL⁻¹
570 as opposed to 10² - 10³ cells mL⁻¹ in this study). With this being the case, the allometric
571 conversions seem most appropriate.
572

573 The tendency for net heterotrophy is not in agreement with studies of glacier surface (e.g.,
574 Tedstone et al., 2017; Williamson et al., 2018, 2020; Cook et al., 2020) and low elevation
575 snowpacks, such as those in the maritime Antarctic (e.g., Gray et al., 2020). However, it is likely
576 that time, more persistent snow cover and nutrient abundance are the key factors limiting the
577 development of autotrophic biomass in the system under study. Furthermore, the snowpack lacked
578 a sufficient autotrophic biomass to start with, with there being virtually none of the so-called snow
579 algae and only modest abundance of cyanobacteria capable of photosynthesis.

580
581

582 **5 Conclusions**

583

584 The present study has been one of the first attempts to thoroughly examine a glacial snowpack
585 ecosystem with respect to its seasonal thermal, biogeochemical and microbial community
586 evolution. The mass balance nutrient data revealed that NH_4^+ and PO_4^{3-} , both essential for
587 biological processes, displayed a non-conservative behaviour (as opposed to Cl^- and NO_3^-), i.e.,
588 they did not follow the expected elution dynamics for a melting snowpack. However, this was not
589 due to sequestration by autotrophic communities, but dust fertilisation and weathering processes
590 that supplemented the winter atmospheric bulk deposition on the ice cap. Indeed, the average
591 autotrophic abundance on the ice cap throughout the melt season was just $0.5 \pm 2.7 \text{ cells mL}^{-1}$.
592 Therefore, the total seasonal biological production within the combined layers of snow and
593 superimposed ice was dominated by bacteria, allometrically estimated at 153 mg C m^{-2} , resulting
594 in a net-heterotrophic (bacterial) snowpack ecosystem. Superimposed ice possessed the same
595 chemical and biological features as the overlying snow, and the percolation of meltwater through
596 the snowpack did not result in any enrichment of nutrients or cells. For the same reason, biological
597 production within the superimposed ice could not be separated from production within the snow.
598 Thus, superimposed ice played a passive role, acting as a temporary dilute storage for nutrients
599 and cells and an effective barrier between the snow and the debris- and cell-rich glacier ice that
600 lay beneath. Bacterial production rates were compared between linear and allometric models of
601 carbon estimation. The latter compared most favourably with studies from the maritime Antarctic
602 and lay in the range 1.2 ± 2 to $1.9 \pm 3.2 \text{ mg C m}^{-2} \text{ day}^{-1}$. However, since autotrophic cells are so
603 much larger than bacterial cells, carbon budgets will be greatly influenced by summers when snow
604 algae are more successful. However, since glacial snowpacks will disappear sooner in a warming
605 climate, they are more likely to be largely net-heterotrophic bacterial ecosystems than autotrophic
606 ecosystems. This is important because fewer nutrients will be assimilated within the snow under
607 these circumstances, and so more will be exported to downstream aquatic ecosystems during early
608 summer.

609

610 **Acknowledgements**

611

612 The author thanks the Commonwealth Scholarship Commission (CSC) for funding through a CSC
613 PhD Scholarship (INCS-2015-214) and the Research Council of Norway BIOICE project (Grant
614 Number 288402). We thank the University Centre in Svalbard (UNIS) students and logistics for
615 their help and support during field work. Imaging work was performed at the Wolfson Light
616 Microscopy Facility (LMF), University of Sheffield under the guidance of Dr. Darren Robinson.
617 Dr. Chris Williamson is thanked for HPLC analysis on the samples.

618 References

- 619
620 Amato, P. *et al.* (2007) 'Bacterial characterization of the snow cover at Spitzberg,
621 Svalbard', *FEMS Microbiology Ecology*, 59(2), pp. 255–264. doi:10.1111/j.1574-
622 6941.2006.00198.x.
623 Amoroso, A. *et al.* (2010) 'Microorganisms in dry polar snow are involved in the
624 exchanges of reactive nitrogen species with the atmosphere', *Environmental Science and
625 Technology*, 44(2), pp. 714–719. doi:10.1021/es9027309.
626 Barbesti, S. *et al.* (2000) 'Two and three-color fluorescence flow cytometric analysis of
627 immunoidentified viable bacteria', *Cytometry*, 40(3), pp. 214–218. doi:10.1002/1097-
628 0320(20000701)40:3<214::AID-CYTO6>3.0.CO;2-M.
629 Bellas, C.M. *et al.* (2013) 'Viral impacts on bacterial communities in Arctic cryoconite',
630 *Environmental Research Letters*, 8(4). doi:10.1088/1748-9326/8/4/045021.
631 Carpenter, E.J., Lin, S. and Capone, D.G. (2000) 'Bacterial Activity in South Pole Snow',
632 *Applied and Environmental Microbiology*, 66(10), pp. 4514–4517.
633 doi:10.1128/AEM.66.10.4514-4517.2000.
634 Cook, J.M. *et al.* (2020) 'Glacier algae accelerate melt rates on the south-western
635 Greenland Ice Sheet', *Cryosphere*, 14(1). doi:10.5194/tc-14-309-2020.
636 Cook, Joseph M. *et al.* (2020) 'Glacier algae accelerate melt rates on the western Greenland
637 Ice Sheet', *The Cryosphere Discussions*, 14(1), pp. 1–31. doi:10.5194/tc-2019-58.
638 Felip, M. *et al.* (1995) *Highly Active Microbial Communities in the Ice and Snow Cover of
639 High Mountain Lakes*, *Applied and Environmental Microbiology*. Available at:
640 <http://aem.asm.org/> (Accessed: 25 September 2018).
641 Felip, M. *et al.* (2007) 'Suitability of flow cytometry for estimating bacterial biovolume in
642 natural plankton samples: Comparison with microscopy data', *Applied and Environmental
643 Microbiology*, 73(14), pp. 4508–4514. doi:10.1128/AEM.00733-07.
644 Fiołka, M.J. *et al.* (2021) 'Morphological and spectroscopic analysis of snow and glacier
645 algae and their parasitic fungi on different glaciers of Svalbard', *Scientific Reports*, 11(1),
646 p. 21785. doi:10.1038/s41598-021-01211-8.
647 Fogg, G.. (1967) 'Observations on the Snow Algae of the South Orkney Islands',
648 *Philosophical Transactions of the Royal Society of London*, 252(777), pp. 279–287.
649 Fujii, M. *et al.* (2010) 'Microbial community structure, pigment composition, and nitrogen
650 source of red snow in antarctica', *Microbial Ecology*, 59(3), pp. 466–475.
651 doi:10.1007/s00248-009-9594-9.
652 Gray, A. *et al.* (2020) 'Remote sensing reveals Antarctic green snow algae as important
653 terrestrial carbon sink', *Nature Communications*, 11, p. 2527. doi:10.1038/s41467-020-
654 16018-w.
655 Grégori, G. *et al.* (2001) 'Resolution of Viable and Membrane-Compromised Bacteria in
656 Freshwater and Marine Waters Based on Analytical Flow Cytometry and Nucleic Acid
657 Double Staining', *Applied and Environmental Microbiology*, 67(10), pp. 4662–4670.
658 doi:10.1128/AEM.67.10.4662-4670.2001.
659 Hamilton, T.L. and Havig, J. (2017) 'Primary productivity of snow algae communities on
660 stratovolcanoes of the Pacific Northwest', *Geobiology*, 15(2), pp. 280–295.
661 doi:10.1111/gbi.12219.
662 Hodson, A., Roberts, T.J., *et al.* (2010) 'Glacier ecosystem response to episodic nitrogen
663 enrichment in Svalbard, European High Arctic', *Biogeochemistry*, 98(1–3), pp. 171–184.

- 664 doi:10.1007/s10533-009-9384-y.
- 665 Hodson, A., Cameron, K., *et al.* (2010) ‘The structure , biological activity and
666 biogeochemistry of cryoconite aggregates upon an Arctic valley glacier : Longyearbreen ,
667 Svalbard’, *Journal of Glaciology*, 56(196), pp. 349–362.
- 668 Hodson, Andy *et al.* (2017) ‘Climatically sensitive transfer of iron to maritime Antarctic
669 ecosystems by surface runoff’, *Nature Communications*, 8, pp. 1–7.
670 doi:10.1038/ncomms14499.
- 671 Hodson, Andrew *et al.* (2017) ‘Microbes influence the biogeochemical and optical
672 properties of maritime Antarctic snow’, *Journal of Geophysical Research: Biogeosciences*,
673 122(6), pp. 1456–1470. doi:10.1002/2016JG003694.
- 674 Hoham, R.W. *et al.* (2006) ‘Two new species of green snow algae from Upstate New York,
675 Chloromonas chenangoensis sp. nov. and Chloromonas tughillensis sp. nov. (Volvocales,
676 Chlorophyceae) and the effects of light on their life cycle development’, *Phycologia*, 45(3),
677 pp. 319–330. doi:10.2216/04-103.1.
- 678 Irvine-Fynn, T.D.L. *et al.* (2012) ‘Microbial cell budgets of an Arctic glacier surface
679 quantified using flow cytometry’, *Environmental Microbiology*, 14(11), pp. 2998–3012.
680 doi:10.1111/j.1462-2920.2012.02876.x.
- 681 Kepner, R.L., Wharton, R.A. and Suttle, C.A. (1998) ‘Viruses in Antarctic lakes.’,
682 *Limnology and oceanography*, 43(7), pp. 1754–1761. doi:10.4319/lo.1998.43.7.1754.
- 683 Krug, L. *et al.* (2020) ‘The microbiome of alpine snow algae shows a speci fi c inter-
684 kingdom connectivity and algae-bacteria interactions with supportive capacities’, *The
685 ISME Journal* [Preprint]. doi:10.1038/s41396-020-0677-4.
- 686 Kühnel, R. *et al.* (2013) ‘Reactive nitrogen and sulphate wet deposition at Zeppelin Station,
687 Ny-Ålesund, Svalbard’, *Polar Research*, 32. doi:10.3402/polar.v32i0.19136.
- 688 Lebaron, P., Parthuisot, N. and Catala, P. (1988) ‘Comparison of blue nucleic acid dyes for
689 the flow cytometry enumeration of bacteria in aquatic systems.’, *Applied and
690 Environmental Microbiology*, 64(5), pp. 1724–1730. doi:<p></p>.
- 691 Michaud, L. *et al.* (2014) ‘Snow surface microbiome on the High Antarctic Plateau
692 (DOME C.)’, *PLoS ONE*, 9(8), p. e104505. doi:10.1371/journal.pone.0104505.
- 693 Mikucki, J.A. and Priscu, J.C. (2007) ‘Bacterial diversity associated with blood falls, a
694 subglacial outflow from the Taylor Glacier, Antarctica’, *Applied and Environmental
695 Microbiology*, 73(12), pp. 4029–4039. doi:10.1128/AEM.01396-06.
- 696 Nowak, A., Hodson, A. and Turchyn, A. V. (2018) ‘Spatial and Temporal Dynamics of
697 Dissolved Organic Carbon, Chlorophyll, Nutrients, and Trace Metals in Maritime
698 Antarctic Snow and Snowmelt’, *Frontiers in Earth Science*, 6, p. 201.
699 doi:10.3389/feart.2018.00201.
- 700 P. Kemp, B. F. Sherr, E. B. Sherr, and J.J.C. (1993) ‘The relation between biomass and
701 volume of bacteria’, in *Handbook of Methods in Aquatic Microbiology*, pp. 303–308.
702 Available at:
703 [https://books.google.co.uk/books?hl=en&lr=&id=ql1ZDwAAQBAJ&oi=fnd&pg=RA1-PA35&dq=Norland,+S.+1993.+The+relationship+between+biomass+and+volume+of+bacteria,+p.+303-307.+In+P.+F.+Kemp,+B.+F.+Sherr,+E.+B.+Sherr,+and+J.+J.+Cole+\(ed.\),+Handbook+of+methods+in+a.](https://books.google.co.uk/books?hl=en&lr=&id=ql1ZDwAAQBAJ&oi=fnd&pg=RA1-PA35&dq=Norland,+S.+1993.+The+relationship+between+biomass+and+volume+of+bacteria,+p.+303-307.+In+P.+F.+Kemp,+B.+F.+Sherr,+E.+B.+Sherr,+and+J.+J.+Cole+(ed.),+Handbook+of+methods+in+a.)
- 704 Posch, T. *et al.* (2001) ‘Precision of bacterioplankton biomass determination: A
705 comparison of two fluorescent dyes, and of allometric and linear volume-to-carbon

- 710 conversion factors', *Aquatic Microbial Ecology*, 25(1), pp. 55–63.
711 doi:10.3354/ame025055.
- 712 Reijmer, C.H. *et al.* (2012) 'Refreezing on the Greenland ice sheet: A comparison of
713 parameterizations', *The Cryosphere*, 6(4), pp. 743–762. doi:10.5194/tc-6-743-2012.
- 714 Rutter, N. *et al.* (2011) 'Hydrology and hydrochemistry of a deglaciating high-Arctic
715 catchment, Svalbard', *Journal of Hydrology*, 410(1–2), pp. 39–50.
716 doi:10.1016/j.jhydrol.2011.09.001.
- 717 Skidmore, M.L., Foght, J.M. and Sharp, M.J. (2000) 'Microbial life beneath a high Arctic
718 glacier', *Applied and Environmental Microbiology*, 66(8), pp. 3214–3220.
719 doi:10.1128/AEM.66.8.3214-3220.2000.
- 720 Stibal, M. *et al.* (2007) 'Seasonal and diel changes in photosynthetic activity of the snow
721 alga *Chlamydomonas nivalis* (Chlorophyceae) from Svalbard determined by pulse
722 amplitude modulation fluorometry', *FEMS Microbiology Ecology*, 59(2), pp. 265–273.
723 doi:10.1111/j.1574-6941.2006.00264.x.
- 724 Stibal, M. *et al.* (2015) 'Microbial abundance in surface ice on the Greenland Ice Sheet.',
725 *Frontiers in Microbiology*, 6(March), p. 225. doi:10.3389/fmicb.2015.00225.
- 726 Takacs, C.D. and Priscu, J.C. (1998) 'Bacterioplankton dynamics in the McMurdo Dry
727 Valley lakes, Antarctica: Production and biomass loss over four seasons', *Microbial
728 Ecology*, 36(3), pp. 239–250. doi:10.1007/s002489900111.
- 729 Takeuchi, N. *et al.* (2006) 'Spatial distribution and abundance of red snow algae on the
730 Harding Icefield, Alaska derived from a satellite image', *Geophysical Research Letters*,
731 33(21), pp. 1–6. doi:10.1029/2006GL027819.
- 732 Tedstone, A.J. *et al.* (2017) 'Dark ice dynamics of the south-west Greenland Ice Sheet',
733 *The Cryosphere*, 11(6), pp. 2491–2506. doi:10.5194/tc-11-2491-2017.
- 734 Tranter, M. and Jones, H.G. (2001) 'The Chemistry of Snow: Processes and Nutrient
735 Cycling', *Snow ecology: An Interdisciplinary Examination of Snow-Covered Ecosystems*,
736 22(6), pp. 127–167.
- 737 Whitman, W.B., Coleman, D.C. and Wiebe, W.J. (1998) 'Prokaryotes: The unseen
738 majority', *Proceedings of the National Academy of Sciences*, 95(12), pp. 6578–6583.
739 doi:10.1073/pnas.95.12.6578.
- 740 Williamson, C.J. *et al.* (2018) 'Ice algal bloom development on the surface of the
741 Greenland Ice Sheet', *FEMS Microbiology Ecology*, 94(3). doi:10.1093/femsec/fiy025.
- 742 Williamson, C.J. *et al.* (2020) 'Algal photophysiology drives darkening and melt of the
743 Greenland Ice Sheet', *Proceedings of the National Academy of Sciences*, pp. 1–12.
744 doi:10.1073/pnas.1918412117.
- 745